Single Molecule Rod−Globule Phase Transition for Brush Molecules at a Flat Interface

Sergei S. Sheiko,*,† Svetlana A. Prokhorova,‡ Kathryn L. Beers,§ Krzysztof Matyjaszewski,§ Igor I. Potemkin,⊥ Alexei R. Khokhlov,⊥ and Martin Möller*,‡

Department of Chemistry, University of North Carolina at Chapel Hill, North Carolina 27599; Organische Chemie III/Makromolekulare Chemie, Universität Ulm, D-89069 Ulm, Germany; Department of Chemistry, Carnegie Mellon University, 4400 Fifth Avenue, Pittsburgh, Pennsylvania 15213; and Physics Department, Moscow State University, 117234 Moscow, Russia

Received April 30, 2001; Revised Manuscript Received August 23, 2001

ABSTRACT: The coexistence of two different conformational states in one molecule has been visualized by scanning force microscopy for a rod−globule transition of brush molecules adsorbed on a water surface. The transition, which occurred upon lateral compression of monolayers, was also examined theoretically by scaling analysis that proved its first-order character. The transition becomes less distinct with decreasing length of the side chains and finally vanishes below a certain critical value.

1. Introduction

Conformational transitions and the corresponding stimuli response of macromolecules provide fundamental means for the molecular assembly and function of biological systems.[1] Establishing a likewise control factor in the field of synthetic macromolecules is recognized as a major challenge in nanotechnology.[2−4] According to theoretical considerations, the transition between the states of expanded coil and compact globule can be discrete, depending on the nature of the interaction and the chain flexibility.[5−9] Equilibrium coexistence of two populations of macromolecules as an unambiguous criterion for a first-order transition[5] has been clearly observed only in the case of relatively large DNA molecules.[9] Here for the first time, we report on a system where such coexistence can be visualized on a significantly smaller length scale in detailed molecular resolution. The peculiar result is the observation that the topology of the branching can provide the competitive interactions necessary for such a transition.

Conformational changes of a brush molecule with a flexible backbone and densely attached flexible side chains, which are adsorbed at an interface, depend on the interplay of the intramolecular and surface forces.[10−13] Interaction of the monomer units with a flat substrate changes the orientation of the side chains relative to the backbone and breaks the symmetry and the dimensionality of the system. One can envision two distinct molecular conformations, in which the free energy is minimized with respect to different contributions. The stretched backbone in Figure 1a is energetically favored and corresponds to a large number of surface contacts of the side-chain monomer units. The globular conformation in Figure 1b is favored entropically by coiling of desorbed side chains at the expense of the number of surface contacts. Since the free energies of these two conformations vary differently with respect to the contact area and interaction strength, the brushes can undergo a phase transition at a certain surface pressure or at a certain spreading coefficient.

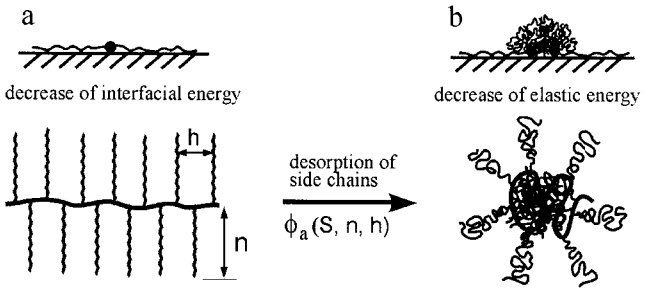

Figure 1. Phase transition from the rodlike (a) to a globule state (b) caused by partial desorption of the side chains. The fraction of adsorbed side chains ϕ_a depends on the spreading coefficient S, the length of the side chains n, and the grafting density h^{-1}.

In this paper, we report on the conformational transition of cylindrical brushes of poly(*n*-butyl acrylate) (PBA) due to lateral compression of a molecular layer on water. When the fraction of adsorbed side chains reduces below a critical value, a discrete transition occurs from an extended conformation to a globular one. We have succeeded in the visualization of individual molecules and the monitoring of their conformational changes by scanning force microscopy (SFM). The transition was analyzed by a scaling approach that proved the first-order character of the transition and its critical dependence on the side chain length.

2. Experimental Section

Materials. A series of three PBA brushes (polymers A, B, and C) differing in the length of the side chains was prepared by grafting of *n*-butyl acrylate from a well-defined poly(2-(2-bromopropionyloxy)ethyl methacrylate) (pBPEM) macroinitiator, which was prepared using atom transfer radical polymerization (ATRP).[14−16] The grafted PBA chains were also prepared by ATRP initiated from the bromopropionate side groups. The concentration of active sites and the conversion of monomer to polymer (typically < 20%) during the polymerization were kept low to reduce the contribution of side

† University of North Carolina at Chapel Hill.
‡ Universität Ulm.
§ Carnegie Mellon University.
⊥ Moscow State University.

10.1021/ma010746x CCC: $20.00
Published on Web 10/30/2001

Table 1. Molecular Characterization of the PBPEM Macroinitiators and the Corresponding PBA Brushes by Multiangle Laser Light Scattering Size Exclusion Chromatography (MALLS-SEC) and Static Light Scattering (SLS)

	macroinitiatior			brush		
polymer	m_w,[a] g/mol	m_w/m_n	N[b]	M_w,[c] g/mol	M_w/M_n[d]	n_{LS}[e]
A	2.2×10^5	1.3	641	4.6×10^6	1.1	48
B	1.6×10^5	1.3	453	1.6×10^6	1.2	20
C	1.8×10^5	1.4	490	1.4×10^6	1.3	15

[a] By MALLS-SEC using $dn/dc = 0.084 \pm 0.042$. [b] Number-average degree of polymerization calculated as $N = m_n/m_0$, where $m_0 = 265$ g/mol (molecular weight of the monomer unit of pBPEM). [c] By SLS using the refractive index increment $dn/dc = 0.068$. [d] Polydispersity from MALLS-SEC. [e] The number-average degree of polymerization of the side chains was determined as $n_{LS} = (M_n - m_n)/NM_0$, where $M_0 = 128$ g/mol (molecular weight of BA) and M_n (number-average molecular weight of the PBA brush measured by MALLS-SEC and SLS).

reactions such as intermolecular coupling. The degrees of polymerization of the main and side chains were controlled by the final concentration of monomer converted to polymer relative to the concentration of initiation sites. A maximum grafting density was achieved because each repeat unit of the backbone contained an initiation site for polymerization. The polymer choice was essential for two reasons. First, PBA has a relatively low glass transition temperature of −54 °C, which favors rapid equilibration of the molecular conformation at room temperature. Second, ATRP yields brushes with a well-defined degree of polymerization of the main chain.

Characterization. Weight- and number-average molecular weights were determined by gel permeation chromatography (GPC) equipped with Waters microstyragel columns (pore size 10^5, 10^4, 10^3 Å) and three detection systems: a differential refractometer (Waters model 410), multiangle laser light-scattering (MALLS) detector (DAWN model F), and a differential viscometer (Viscotek model H502). The measurements were conducted in THF (25 °C) at a flow rate of 1 mL/min. The setup was calibrated against low-polydispersity poly(methyl methacrylate) (pMMA) or polystyrene (pS) standards (PSS, Germany). The refractive index increment dn/dc was determined in THF at 25 °C with an Otsuka Photal RM-102 differential refractometer.

Langmuir−Blodget Films. Monolayers were prepared at ambient conditions using a 750 cm^2 rectangular trough (FW2, Lauda) filled with double-distilled water (Mili-Q plus 185). After a 200 μL portion of a dilute solution of brushes in chloroform ($c = 1$ mg/mL) was deposited on the water surface, compression at a speed of 35 cm^2/min was initiated at a 30 min delay, so as to allow even spreading of brush molecules. The surface pressure was measured at 21 °C using a barrier/pressure transducer with a precision of 0.3 mN/m. Monolayers at different compression degrees were transferred onto a mica substrate for SFM measurements. During the film transfer, the pressure was maintained constant.

Scanning Force Microscopy. Scanning force micrographs were recorded with a Nanoscope IIIa instrument (Digital Instruments, St. Barbara, CA) operating in the tapping mode. The measurements were performed at ambient conditions (in air, 56% relative humidity, 27 °C) using Si cantilevers with a spring constant of ≈50 N/m, a tip radius of 8 nm, and a resonance frequency of about 300 kHz. The set-point amplitude ratio was maintained at 0.9 to minimize the sample deformation induced by the tip.

Special software was developed for determination and analysis of the in-plane conformation of the adsorbed molecules visualized by SFM. The coordinates of the molecular contour were determined by dragging a cursor along the contour and automatically recording the point coordinates. The program enabled statistical evaluation of different molecular dimensions, such as the contour length, the radius of gyration, the end-to-end distance, and the persistence length. The molecular dimensions were averaged for a large ensemble of molecules (>200) to ensure accuracy within a statistical error of 5%.

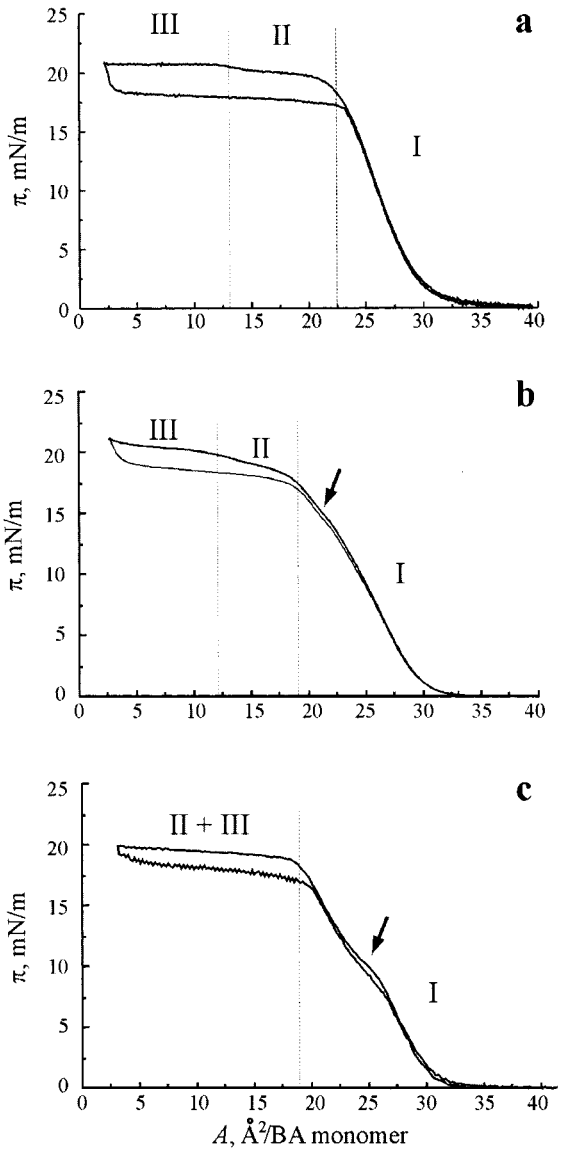

Figure 2. Compression−expansion isotherm for PBA brushes with different length of the side chains: (a) polymer A, $n = 48$; (b) polymer B, $n = 20$; and (c) polymer C, $n = 15$. Regions I, II, and III correspond to the pressure raise, the first plateau, and the second plateau, respectively. The arrows in (b) and (c) indicate the inflection point of unknown nature.

3. Results and Discussion

3.1. Experimental Results. a. Compression Isotherm. From the total molecular weight, the number-average degree of polymerization of the side chains was calculated to be 48, 20, and 15 for polymers A, B, and C, respectively (Table 1). Owing to the amphiphilic nature of *n*-butyl acrylate groups, the brushes spread readily on the water surface. Figure 2a shows a $\pi-A$ (surface pressure vs film area per BA residue) isotherm for polymer A with the longest side chains. Similar to other fluids, compression of the PBA brushes was reversible as expected for equilibrium spreading. However, it exhibited distinct features that were not typical for conventional liquids. The pressure onset occurred at about 35 $Å^2$ and rose until a critical area of 22 $Å^2$, at which the pressure leveled off at 19.5 mN/m. The plateau between 22 and 13 $Å^2$ was followed by a second

Table 2. Molecular Dimensions of PBA Brushes in Uncompressed Monolayers Determined from SFM Micrographs and Averaged for an Ensemble of More Than 200 Molecules

	L_n,[a] nm	D,[b] nm	A,[c] nm^2	$\langle R_g \rangle$,[d] nm	l_p,[e] nm	n_{SFM}[f]	λ[g]
A	149	45	8850	39/30	312/30	49	212
B	103	24	3352	24/21	75/33	26	116
C	112	12	2369	24/25	40/35	17	75

[a] Number-average length of brush molecules (±6 nm). [b] Average distance between backbones. [c] Average area per brush molecule. [d] Mean-square radius of gyration was measured prior to compression and after expansion, respectively (prior/after). [e] Persistence length is a characteristic length in the correlation function $\langle \cos(\Theta) \rangle = e^{-l/l_p}$ for the average cosine angle between the tangents along the brush molecule separated by distance l. [f] Number-average degree of polymerization of PBA side chains determined as $n = A/(Na_0)$, where $a_0 = 28$ Å^2 area per BA monomer unit of the transferred monolayers. [g] $\lambda = A/(a_0 L_n)$ = linear density of the "surface stickers" (BA monomer units) per unit length of the brush.

plateau with a distinct increase in pressure from 19.5 to 21 mN/m. The other distinct feature was hysteresis, which was observed on compressions beyond the first plateau. In the range of molecular areas above 13 Å^2 (the end of the first plateau), expansion occurred without hysteresis.

Polymer B demonstrated a similar behavior (Figure 2b). It also showed two plateaus: (i) in the range from 19 to 12 Å^2, where the pressure slightly increased from 17.5 to 19.5 mN/m, and (ii) from 12 to 5 Å^2 at pressure around 21 mN/m. Compared to polymer A, the first plateau of polymer B was less distinct. Another difference between polymers A and B was observed in region I, where the isotherms revealed a subtle inflection at about 21 Å^2 as shown by the arrow in Figure 2a. The origin of this inflection, which was also observed for polymer C, is not clear yet and will not be discussed in this paper. Polymer C, which had the shortest side chains, demonstrated a completely different behavior (Figure 2c). In contrast to polymers A and B, the polymer revealed only one plateau at 21 mN/m, while the inflection in range I became more pronounced.

For all three polymers, linear extrapolation of the isotherms to zero pressure gave the area $a_0 = 29 \pm 1$ Å^2, which was consistent with the monomer area of 29.3 Å^2 measured for linear PBA.[17,18] Also, the pressure in the plateau region $\pi = 21$ mN/m was similar to that of linear PBA (22 mN/m). On the basis of numerous PBA studies, we assume that essentially all ester groups of the BA repeat units of the brush molecules are in contact with the water surface and the butyl tails are oriented toward air.

b. Visualization of Individual Molecules. Single brush molecules as adsorbed on a solid substrate are shown in Figure 3. In this unique micrograph one can even distinguish the individual side chains as tiny hairs at the periphery of the corona. The investigation of single brush molecules has been discussed elsewhere.[19] To visualize conformational changes caused by the lateral compression, monolayers were transferred to a mica substrate (transfer ratio 97%) and imaged by SFM. Figure 4 shows a series of tapping mode micrographs (height contrast) obtained from polymers A, B, and C at different compression degrees. Prior to compression, i.e., transferred onto mica at low pressure (1 mN/m), brush molecules were resolved as individual wormlike structures lying parallel to the substrate plane (Figure 4-a1,b1,c1). The white threads correspond to the backbone, whereas the area between the threads is covered by extended side chains. This interpretation was verified by SFM of single molecules that revealed a uniform corona of the side chains around the backbones (Figure 3).

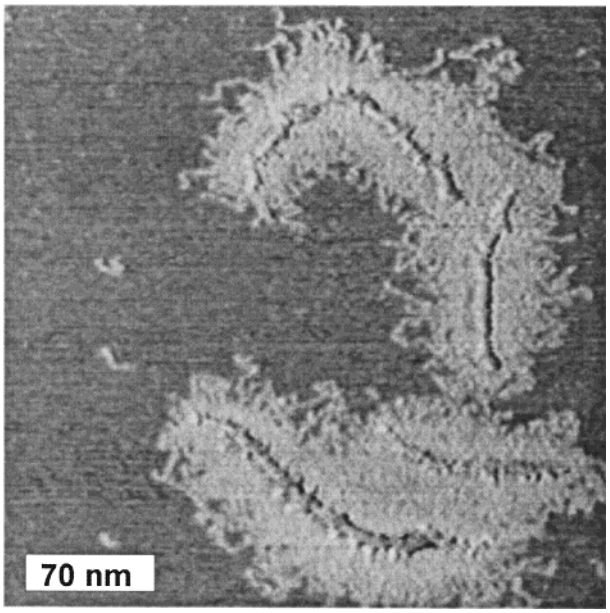

Figure 3. SFM micrograph of single molecules of PBA brushes (polymer A) on mica, which were prepared by spin-casting of a dilute solution in chloroform.

The most important observations are related to morphological changes caused by the lateral compression. Polymers A and B demonstrated a transition from the rodlike to a globular conformation as depicted in Figure 4-a1−a4 and Figure 4-b1−b4, respectively. Furthermore, the transition in polymer A proceeds through a coexistence range (Figure 4-a3), where both conformations occur at constant pressure and temperature, in some cases within the same molecule. Polymer B also demonstrated a steep transition from the extended to the coiled conformation; however, the coexistence regime in Figure 4-b4 was less pronounced. In contrast, polymer C did not exhibit any significant changes in molecular conformation even in the plateau range. At areas below 18 Å^2, the molecules were retracted from the water surface as a whole and squeezed upward to form an additional layer. Ill-defined aggregates were visualized by SFM as white elevations in Figure 4-c4.

One must noted that the structure of the Langmuir films might change during their transfer on the solid substrate. On the basis of the following arguments, we believe that the observed molecular conformations correspond to those at the water−air interface. (i) The observed transition from rods to globuli is consistent. During the transition from rods to globuli, the total number of molecules remains constant, while the number of globuli and the number of rods progressively increases and decreases, respectively. (ii) The transition is fully reversible. One obtains the same fractions of rods and globuli upon compression and expansion to a given molecular area. (iii) Annealing of the transferred films in Figure 4-a4,b4,c4 resulted in aggregation of individual molecules into larger droplets. The fact that annealing drove the system to a completely different morphology is indicative for the structures, which were formed at the air−water interfaces and then quenched by transfer to the solid substrate. (iv) Adsorption of brush molecules on mica directly from solution gave

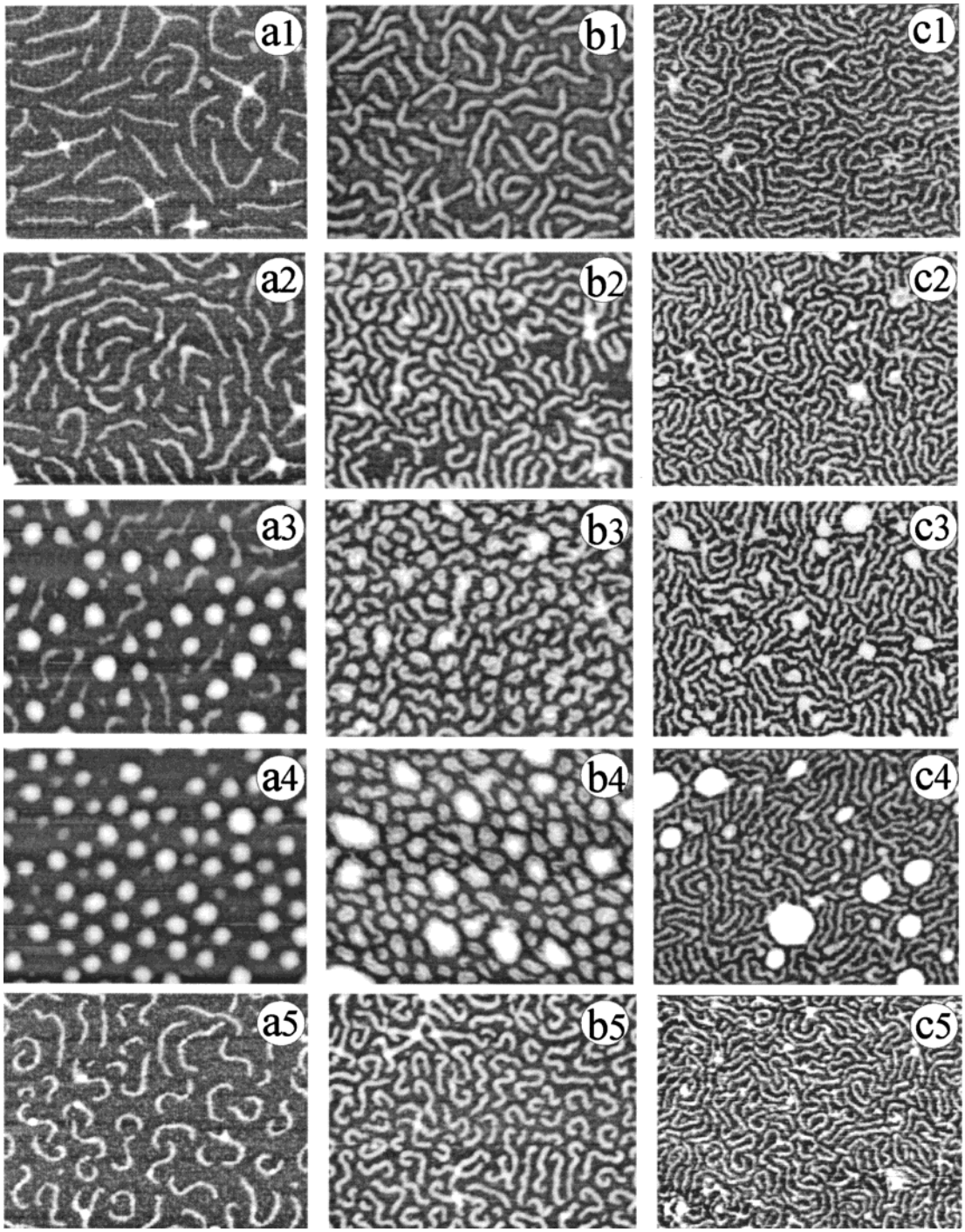

Figure 4. SFM micrographs (600 × 400 nm^2) of monolayers of PBA brushes (A: a1−5, B: b1−5, C: c1−5) transferred on mica at different degree of compression: (a1,b1,c1) 31 Å^2, (a2,b2,c3) 21 Å^2, (a3,b3,c3) 17 Å^2, (a4,b4,c4) 13 Å^2, (a5,b5,c5) 31 Å^2 (after expansion).

extended coil conformations in Figure 3, which were similar to those of the Langmuir−Blodgett films prior to compression (Figure 4-a1,b1,c1).

c. Molecular Conformation. The SFM micrographs enabled statistical evaluation of molecular dimensions, such as the axial length, the radius of gyration, and the apparent persistence length (Table 2). From the area per brush molecule (A) and the degree of polymerization of the backbone (N) one can estimate the number-average degree of polymerization of the side chains (n_{SFM}). The values were in remarkable agreement with n_{LS} determined independently by light scattering (Table 1). Moreover, the number-average brush length (L_n) gives the length per monomer unit $l_m = L_n/N$ to be 0.23, 0.23, and 0.25 nm for polymers A, B, and C, respectively. These values are consistent with the projected monomer unit length $l_0 = 0.25$ nm of a carbon chain in the all-trans zigzag conformation. From this comparison we can conclude that within the 10% accuracy of the experiment the main chain of the brushes is almost fully stretched. Some of the entries in Table 2 contain two values, which correspond to molecular dimensions obtained at the same $\pi(A)$ values before and after the first compression−expansion cycle. The succeeding cycles did not show any significant difference between compression and expansion morphologies measured at the same degree of compression.

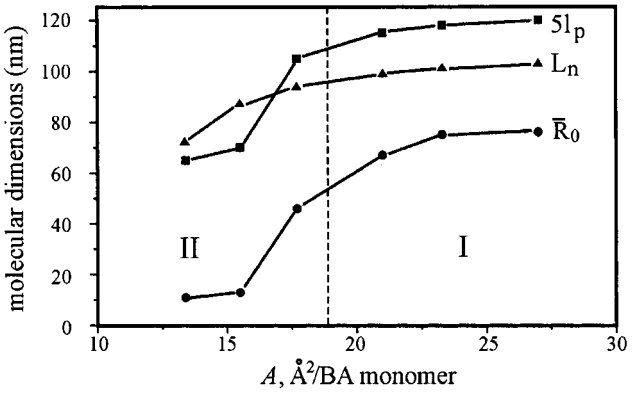

Figure 5. Variation of molecular dimensions of polymer B with the film area: (●) end-to-end distance $\langle R_0^2\rangle^{1/2}$, (■) persistence length l_p depicted as $5l_p$, and (▲) the number-average contour length L_n. Regions I and II correspond to the pressure−area isotherm in Figure 2b.

Other important correlations in Table 2 regard the interchain distance $D \sim n$ and the persistence length $l_p \sim n^{2.7\pm0.3}$. However, here we will focus only on those changes that are relevant to the conformational transition. The most complete information was collected for polymer B, for which the backbone was resolved through the whole transition interval. Figure 5 depicts variation of different molecular dimensions as a function of the film area per BA monomer. In the range above 19 Å^2, only small changes were observed. Significant changes in the molecular structure occurred in the plateau range from 19 to 12 Å^2. All three parameters, i.e., the end-to-end distance $\langle R_0^2\rangle^{1/2}$, the persistence length l_p, and the apparent contour length L_n, demonstrated a drastic decrease within a relatively small interval of compression.

3.2. Scaling Analysis. a. Theoretical Background. The observed conformational transition was analyzed theoretically assuming partial desorption of the side chains (i) upon variation of the spreading coefficient and (ii) under lateral compression. In the uncompressed state (Figure 4-a1,b1,c1), strong adsorption leads to extension of the brush molecule due to interaction of the side chains, which are confined to the surface plane. Decreasing of the surface area makes a fraction of the side chains desorb and aggregate to a 3D globule (Figures 4-a4 and 4-b4). Therefore, the free energy F of the adsorbed brush in a poor solvent results from a balance of the interfacial energy, which decreases upon adsorption, and the elastic energy, which decreases upon desorption:

$$F = F_{el}^{2D} + F_{el}^{3D} + F_s + F_{mix} \qquad (1)$$

On a short length scale, the shape of the brush molecule on a flat surface can be presented as a cylindrical aggregate of N_{3D} desorbed side chains surrounded by a monolayer of N_{2D} adsorbed chains (Figure 6). The length L and the radius r of the cylinder correspond to the longitudinal dimension of the brush molecule and the end-to-end distance of the desorbed side chains, respectively. The width R and the thickness a of the monolayer correspond to the end-to-end distance of adsorbed side chains and to the molecular size, respectively. Since the adsorbed side chains and the backbone are almost fully stretched, their conformation strongly deviates from the Gaussian one. For the freely jointed chain model, the chain stretching can be represented via the Langevin function as $R = an(\coth p_s - 1/p_s)$, $L = aN(\coth p_b - 1/p_b)$, where $N = N_{2D} + N_{3D}$ is the total number of the side chains and n is the number of Kuhn segments in the side chain.[20] The elastic forces $p_s = f_s a/kT$ and $p_b = f_b a/kT$ represent normalized (dimensionaless) forces, which are derived from the forces f_s and f_b applies to the ends of the side chain and the backbone, respectively. The elastic energy F_{el}^{2D} of the adsorbed brush can be derived as a result of action of the forces p_s and p_b:

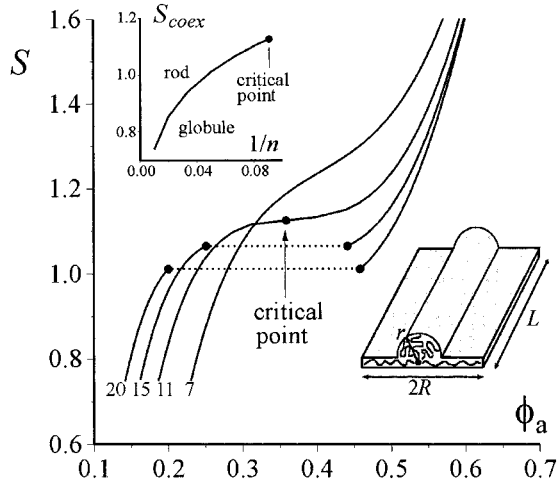

Figure 6. Spreading coefficient S vs fraction of adsorbed side chains $\phi_a = N_{2D}/N$ for different values of the side chain length $n = 7$, 11, 15, and 20. The dotted lines show discontinuous phase transitions from the globular to the rodlike conformation. The insert depicts the dependence of the spreading coefficient S_{coex} at coexistence of the two conformations on the side chain length.

$$F_{el}^{2D}/kT = N_{2D}n\left(p_s \coth p_s - 1 - \ln\frac{\sinh p_s}{p_s}\right) + N\left(p_b \coth p_b - 1 - \ln\frac{\sinh p_b}{p_b}\right) \qquad (2)$$

The first term in eq. 2 gives the elastic free energy for N_{2D} side chains, whereas the second term corresponds to the backbone. In contrast, the elastic energy of N_{3D} desorbed side chains has the conventional Flory form $F_{el}^{3D}/kT = N_{3D}r^2/na^2$, which gives linear dependence for the stretching force. Note that F_{el}^{3D} is a limiting case of the elastic energy of the adsorbed side chains, which corresponds to small relative extensions ($r \ll na$ and $p_s \ll 1$) of the desorbed side chains.

The surface energy of the adsorbed brush depends on the molecular dimensions L, R, and r as

$$F_s = \gamma_{12}A_1 + \gamma_1(A_0 - A_1) + \gamma_2(A_2 + A_1) \cong \text{const} + \gamma_2 Lr - SLR \qquad (3)$$

where $A_1 \cong LR$ and $A_2 \cong Lr$ are the areas of the adsorbed 2D layer and 3D cylindrical aggregate of the desorbed side chains, respectively; A_0 is the area of water/air surface per molecule which is constant. S is the spreading coefficient $S = \gamma_1 - \gamma_{12} - \gamma_2$, where γ_1, γ_{12}, and γ_2 are the interfacial energies of the water/air, water/polymer, and polymer/air interfaces, respectively. In the surface energy term, we omitted contributions due to the long-range van der Waals forces and due to variations of the monolayer surface energy upon perpendicular orientation of the butyl groups with respect

to the water surface. In the regime of strong adsorption, these two contributions are negligible compared to the short-range surface interactions and the tremendous elastic energy stored in the extended brush molecules. In fact, the effect of the van der Waals forces was observed at higher degrees of compression when large droplets on top of the brush monolayer were detected. This corresponds to the regime of pseudo partial dewetting,[21] which is consistent with the negative Hamaker constant and positive spreading coefficient of a PBA film on water.

The last contribution to the free energy is the mixing entropy of the side chains:

$$\frac{F_{\text{mix}}}{kT} = N_{2D}\ln(N_{2D}/N) + N_{3D}\ln(N_{3D}/N) \qquad (4)$$

The space-filling conditions for the adsorbed layer (2D) and the desorbed side chains (3D) were calculated assuming dense packing of monomer units

$$LR \approx N_{2D}na^2\ (N_{2D}n \gg N) \quad \text{and} \quad Lr^2 \approx N_{3D}na^3 \qquad (5)$$

The assumption of the dense packing is consistent with the molecular area $a_0 = 29 \pm 1$ Å^2 per BA monomeric unit and with the fact that the average distance between the chains is proportional to the side chain length (Table 2). Therefore, at both surface energy and external pressure variation, the density-dependent contribution of intermolecular interactions of brush molecules in the film is constant at and thus can be omitted in the total free energy.

Using the space-filling conditions (5) the total free energy (1) of the brush molecule in monolayer, can be written as a function of two independent variables, e.g., (i) the fraction of adsorbed side chains $\phi_a = N_{2D}/N$ and (ii) the relative length of the brush $x = L/aN$

$$\frac{F}{kTN} = \phi_a n\left(p_s \coth p_s - 1 - \ln\frac{\sinh p_s}{p_s}\right) + \left(p_b \coth p_b - 1 - \ln\frac{\sinh p_b}{p_b}\right) + \frac{3(1-\phi_a)^2}{2x} + \gamma_2\sqrt{xn(1-\phi_a)} - Sn\phi_a + \phi_a \ln \phi_a + (1-\phi_a)\ln(1-\phi_a) \qquad (6)$$

Here, γ_2 and S are introduced as dimensionless parameters multiplied by a^2/kT, where a is the molecular size. The parameters p_s and p_b are related to ϕ_a and x as

$$\frac{\phi_a}{x} = \coth p_s - 1/p_s, \quad x = \coth p_b - 1/p_b \qquad (7)$$

b. Conformational Phase Transition upon Variation of the Spreading Coefficient. An equilibrium value of the total free energy is found by minimization of eq 6 with respect to ϕ_a and x. For long side chains (large n), the free energy revealed two minima: one of them corresponds to the extended brush with a large fraction of adsorbed side chains, while the second minimum corresponds to the collapsed globule with smaller x (axially contracted backbone) and ϕ_a. The resulting dependence $\phi_a(S)$ in Figure 6 demonstrates a discontinuous phase transition from one state to the other. The transition is of first order and exhibits dependence of the side chain length. At longer n, the transition is more distinct and results in significant changes in the number of adsorbed side chains. If the length of the side chains is below a critical value, only gradual conformational changes should be observed.

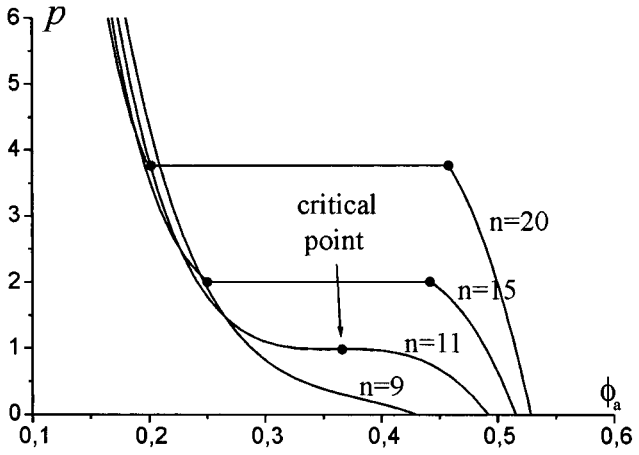

Figure 7. Surface pressure p as a function of the fraction of adsorbed side chains $\phi_a = N_{2D}/N$ was calculated for different values of the side chain length $n = 9$, 11, 15, and 20 at the constant spreading coefficient $S = 1.2$.

On strong adsorption (large S), the minimum of the free energy is attained at $\phi_a \cong 1$ and $x \cong 1$. In this case, the space-filling condition for the adsorbed side chains, eq 5, gives linear dependence of the end-to-end distance R on the side chain length, $R \cong an$. In the opposite case of smaller values of S and ϕ_a ($\phi_a \ll 1$), only two terms give main contribution to the free energy (6): elastic energy of the desorbed side chains and surface energy of their contacts with air, $F/kTN \cong 3/2x + \gamma_2\sqrt{xn}$. A tendency to minimize surface area of the desorbed side chains results in longitudinal contraction of the brush molecule, $x \approx 1/(n^{1/3}\gamma_2^{2/3})$, and stretching of the side chains, $r \approx an^{2/3}\gamma_2^{1/3}$. Note that in this case intermolecular aggregation of the desorbed side chains in the monolayer is hindered by a small fraction of the adsorbed side chains.

c. Conformational Phase Transition under Lateral Compression. Theoretical analysis of the phase transition upon variation of the spreading coefficient can be extended for the description of a real experimental situation when lateral compression results in conformational changes at constant S. In theoretical consideration this pressure can be defined as a derivative of the total free energy per brush molecule (eq 1) with respect to the area $A = a^2Nn\phi_a$ occupied by the molecule, i.e., with respect to the fraction of adsorbed side chains ϕ_a.

Figure 7 depicts dimensionless surface pressure $p = \pi na^3/k_BT$ vs fraction of adsorbed side chains ϕ_a for different lengths n of the side chains. Similar to the phase behavior at the variable spreading coefficient, the molecules with relatively short side chains, whose length is below the critical value, exhibited only gradual increase of the pressure under lateral compression. In contrast, brush molecules with longer side chains revealed coexistence of two conformations at constant pressure. At lower degrees of compression, one observes the rodlike conformation, which corresponds to a larger fraction of adsorbed side chains. The onset of the globular conformation was observed above a certain surface pressure, at which drastic desorption of the side chains occurred.

The scaling results are fairly consistent with the experimental observations. In the pressure−area diagrams (Figure 2), polymer A revealed the well-defined plateau, which became less pronounced for polymer B and completely vanished for polymer C. Accordingly, SFM enabled pictorial visualization of both conformations for polymer A in the plateau region (Figure 4-a3); it showed very weak coexistence for polymer B (Figure 4-b3) and almost no conformational changes for polymer C (Figure 4-c3). In the latter case, the lateral compression resulted in desorption of the brush molecules as a whole.[22] The complete desorption of brushes C has occurred due to the significantly smaller number of polar functional groups per unit length of the backbone (λ in Table 2).

4. Conclusions

In conclusion, a peculiar transition from a rodlike to a globular conformation of individual molecules was observed. On the basis of the coexistence of both conformations at constant pressure and temperature and a scaling analysis of the molecular conformation, the transition is proved to be a first-order phase transition. So far, we have not discussed two important aspects which are relevant to the experiment: (i) the effect of intermolecular interactions and monolayer ordering and (ii) the equilibrium conformation of 2D brushes. The scaling analysis showed[23] that coiled conformations in Figure 4-a1,b1,c1 correspond to a deeper minimum, while extended conformations in Figure 4-a5,b5,c5 are in a metastable state. Since these results do not change the fundamental nature of the observed transition, they are omitted in the present paper and will be discussed elsewhere.

Acknowledgment. This work was supported by the German Science Foundation (SFB 569), National Science Foundation, and ATRP Consortium at CMU. K.M. thanks the Humbolt Foundation for a Research Award for US Senior Scientists. I.I.P. and A.R.Kh. are grateful to the Russian Foundation for Basic Research and INTAS for financial support. The authors acknowledge contribution of D. G. Shirvanyants, who developed software for analysis of the in-plane conformation of the adsorbed molecules.

References and Notes

(1) Volkenstein, M. V. *Molecular Biophysics*; Academic Press: New York, 1977.
(2) Stayton, P. S.; Shimoboji, T.; Long, C.; Chilkoti, A.; Chen, G.; Harris, J. M.; Hoffman, A. S. *Nature* **1995**, *378*, 472.
(3) Mao, C.; Sun, W.; Shen, Z.; Seeman, N. C. *Nature* **1999**, *397*, 144.
(4) Montemagno, C.; Bachand, G.; Stelick, S.; Bachand, M. *Nanotechnology* **1999**, *19*, 225.
(5) Lifshitz, I. M.; Grosberg, A. Yu.; Khokhlov, A. R. *Rev. Mod. Phys.* **1978**, *50*, 683.
(6) Swislow, G.; Sun, S.-T.; Nishio, I.; Tanaka, T. *Phys. Rev. Lett.* **1980**, *44*, 796.
(7) Park, I. M.; Wang, Q.-W.; Chu, B. *Macromolecules* **1987**, *20*, 1965.
(8) Ueda, M.; Yoshikawa, K. *Phys. Rev. Lett.* **1996**, *77*, 2133.
(9) Yoshikawa, K.; Takahashi, M.; Vasilevskaya, V. V.; Khokhlov, A. R. *Phys. Rev. Lett.* **1996**, *76*, 3029.
(10) Saariaho, M.; Ikkala, O.; ten Brinke, G. *J. Chem. Phys.* **1999**, *110*, 1180.
(11) Khalatur, P.; Khokhlov, A. R.; Prokhorova, S. A.; Sheiko, S. S.; Möller, M.; Reineker, P.; Shrirvanynts, D.; Starovoitova, N. *Eur. Phys. J. E* **2000**, *1*, 99.
(12) Prokhorova, S. A.; Sheiko, S. S.; Mourran, A.; Möller, M.; Beginn, U.; Zipp, G.; Ahn, C.-H.; Percec, V. *Langmuir* **2000**, *16*, 6862.
(13) Potemkin, I. I.; Khokhlov, A. R.; Reineker, P. *Eur. Phys. J. E* **2001**, *4*, 93.
(14) Beers, K. L.; Gaynor, S. G.; Matyjaszewski, K.; Sheiko, S. S.; Möller, M. *Macromolecules* **1998**, *31*, 9413.
(15) Patten, T. E.; Matyjaszewski, K. *Adv. Mater.* **1998**, *10*, 901.
(16) Matyjaszewski, K. *Chem. Eur. J.* **1999**, *5*, 3095.
(17) Crisp, D. J. *J. Colloid Sci.* **1946**, *1*, 49.
(18) Li, S.; Hanley, S.; Khan, I.; Varshney, S. K.; Eisenberg, A.; Lennox, R. B. *Langmuir* **1997**, *9*, 22243.
(19) Sheiko, S. S.; Möller, M. *Top. Polym. Chem.* **2000**, *212*, 137.
(20) James, H. M.; Guth, E. *J. Chem. Phys.* **1943**, *11*, 455.
(21) Brochard-Wyart, F. *Langmuir* **1991**, *7*, 335.
(22) Ahrens, H.; Hugenberg, N.; Schmidt, M.; Helm, C. A. *Phys. Rev. E* **1999**, *60*, 4360.
(23) Potemkin, I. I.; Khokhlov, A. R. In *Proceedings of the Discussion Meeting on Multi-Level Ordering*, Weingarten, Germany, June 2000; p 18.

MA010746X